

Accepted Manuscript

Title: Hydrothermal combustion synthesis and characterization of Sr_2CeO_4 phosphor powders

Authors: Yanfei Yang, Xiangyu Zuo, Shi Shikao, Jibiao Li, Jiye Wang, Lina Geng, Lianshe Fu



PII: S0025-5408(18)32992-1
DOI: <https://doi.org/10.1016/j.materresbull.2018.12.018>
Reference: MRB 10319

To appear in: *MRB*

Received date: 20 September 2018
Revised date: 11 December 2018
Accepted date: 15 December 2018

Please cite this article as: Yang Y, Zuo X, Shi S, Li J, Wang J, Geng L, Fu L, Hydrothermal combustion synthesis and characterization of Sr_2CeO_4 phosphor powders, *Materials Research Bulletin* (2018), <https://doi.org/10.1016/j.materresbull.2018.12.018>

This is a PDF file of an unedited manuscript that has been accepted for publication. As a service to our customers we are providing this early version of the manuscript. The manuscript will undergo copyediting, typesetting, and review of the resulting proof before it is published in its final form. Please note that during the production process errors may be discovered which could affect the content, and all legal disclaimers that apply to the journal pertain.

Hydrothermal combustion synthesis and characterization of Sr₂CeO₄ phosphor powders

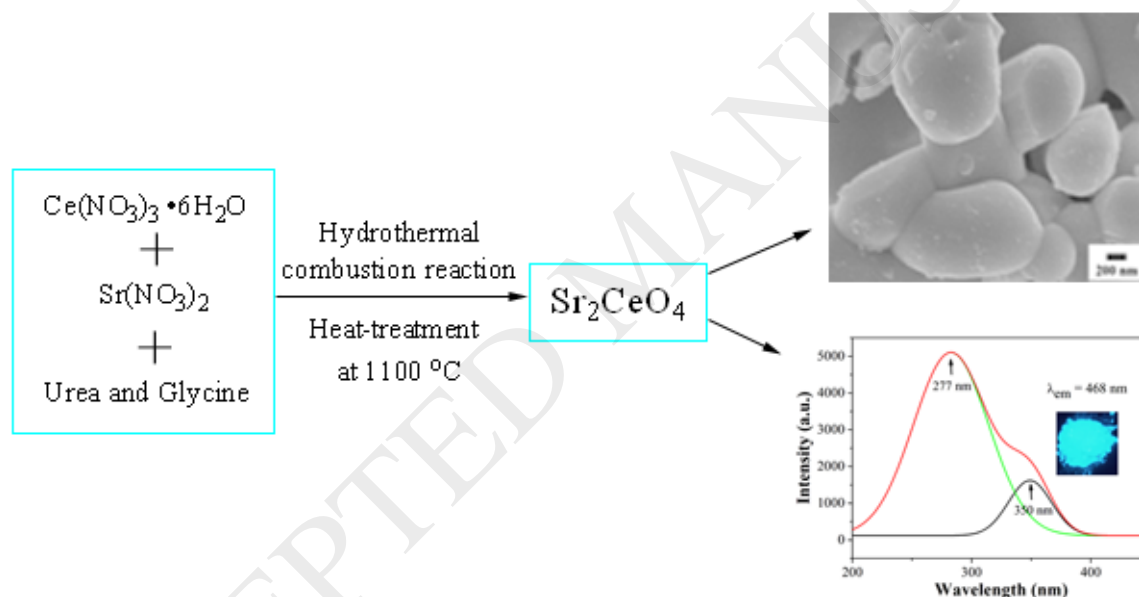
Yanfei Yang ^a, Xiangyu Zuo ^a, Shikao Shi ^{a,*}, Jibiao Li ^a, Jiye Wang ^a, Lina Geng ^a, Lianshe Fu ^b

^aCollege of Chemistry and Materials Science, Key Laboratory of Inorganic Nanomaterials of Hebei Province, Hebei Normal University, Shijiazhuang 050024, P. R. China

^bPhysics Department and CICECO - Aveiro Institute of Materials, University of Aveiro, 3810-193 Aveiro, Portugal

*Corresponding author, Tel: +86-311-80787402, E-mail address: shishikao@hebtu.edu.cn

Graphical abstract



Highlights

- The Sr₂CeO₄ fine powders were prepared by hydrothermal combustion reaction.
- The crystallization, morphology and luminescence can be effectively improved.
- The molar ratio of urea to Gly and sintering temperature are two important factors.
- The optimized samples exhibit spherical shape and uniform size (200~350 nm).
- Intense blue-light emission can be noticed as excited with medium and near UV light.

Abstract In this paper, the blue-light-emitting Sr_2CeO_4 phosphor powders were prepared by hydrothermal combustion reactions and a subsequent sintering process. During the process, the mixed urea and glycine were both used as leavening agent and fuel. The particle crystallization, surface morphology as well as the luminescence intensities of the Sr_2CeO_4 phosphor powders were effectively improved by adjusting the amount of glycine and post-sintering temperatures. The Sr_2CeO_4 phosphor exhibited strong crystallization and well-distributed spherical particle after optimization. Moreover, the intense blue-light emission band with the maximum at 468 nm in the range of 400 to 600 nm was observed as excited with ultraviolet light 277 nm. In particular, after the precursors were heat-treated at 1100 °C, the samples could be well-excited around 350 nm. The excitation bands were ascribed to the charge transfer from O to Ce, and the enlarged excitation range may facilitate its uses in optoelectronic fields.

Keywords: A. Oxides. A. Optical materials. B. Luminescence. D. Phosphor.

1. Introduction

Due to the high thermal and chemical stability, the oxide-based phosphor powders have been given much interests and widely used in diverse optoelectronic devices such as plasma display panels, field emitters, light-emitting diodes and scintillator panels for X-ray radiography [1,2]. Among the oxide-based phosphors, the powders with blue-light emission are very important because they can mix with red, orange and green phosphors in a certain portion to achieve other colors. In general, the blue-light-emitting powders such as $\text{BaMgAl}_{10}\text{O}_{17}:\text{Eu}^{2+}$ are prepared by reducing lanthanide Eu^{3+} to Eu^{2+} , which needs high calcination temperature (1400–1600 °C) accompanied with a reduction atmosphere [3]. At the end of the 20th century, Danielson and his group developed an unusual blue-light-emitting Sr_2CeO_4 material by combinatorial chemistry for the first time [4,5], and then the studies on the phosphor system have attracted great attention owing to its special structure as well as excellent luminescent performance [6,7]. The structure of Sr_2CeO_4 is indexed to an orthorhombic unit cell (space group: Pbam) with one-dimensional chains of edge-sharing CeO_6 octahedrals. The blue-light emission in Sr_2CeO_4 originates from a ligand-to-metal Ce^{4+} charge transfer, which is not related to Ce^{3+} . Thus, it is only necessary to

calcine the raw materials in air without reducing Ce^{4+} to Ce^{3+} in the preparation process. Moreover, the energy transfer from O–Ce band to luminescent lanthanide ions (such as Eu^{3+} and Sm^{3+}) can easily happen after the lanthanide ions are introduced to Sr_2CeO_4 , and the emitting-color is changed from blue to red by adjusting the concentration of lanthanide ions [8-10].

During the past twenty years, some approaches to synthesize Sr_2CeO_4 phosphor powders have been attempted, including the traditional solid state reaction, sol-gel method [11], solution combustion synthesis [12], spray pyrolysis [13], microwave-assisted solvent thermal method [14], co-precipitation reaction [15], high temperature mechano-chemical means [16] and emulsion liquid membrane system [17]. The above approaches often require high temperature, long reaction duration or sophisticated devices. Although the direct solution combustion synthesis is very simple to achieve Sr_2CeO_4 , the as-prepared samples often display serious agglomeration owing to the instantaneous reaction process, and therefore result in irregular distribution, which is certainly to limit its practical applications in optoelectronic fields. In this work, the precursor powder of Sr_2CeO_4 was prepared by a hydrothermal combustion process. During the hydrothermal combustion reaction, the mixed organic composition urea and glycine (abbreviated as Gly) were both used as leavening agent and fuel. It has been found that the particle crystallization, surface morphology and luminescence intensities of the Sr_2CeO_4 phosphor powders were effectively improved by adjusting the amount of Gly and subsequent sintering temperature. In the post-sintering process, it is not necessary to use a reduction atmosphere, and the optimized sintering temperature to achieve the fine Sr_2CeO_4 powder is only 1100 °C, which is much lower than 1400–1600 °C. Moreover, the blue-light-emitting Sr_2CeO_4 sample can be effectively excited with 277 and 350 nm, which is possible to promote its applications in field emission displays and other optoelectronic fields.

2. Experimental

2.1. Synthesis of Sr_2CeO_4 phosphor powders

The initial materials for preparing the Sr_2CeO_4 powders contain $\text{Sr}(\text{NO}_3)_2$ (Yongda Chemical, Tianjin, 99.5%), $\text{Ce}(\text{NO}_3)_3 \cdot 6\text{H}_2\text{O}$ (Yongda Chemical, Tianjin, 99.5%), urea (Analytical Reagent) and Gly (Biochemical Reagent). First of all, the initial materials were mixed together in which the molar ratio of $\text{Sr} : \text{Ce} : \text{urea} : \text{Gly} = 2 : 1 : 5 : x$ ($x = 0-5$), and dissolved with certain amount of distilled water. Then, the aqueous solution was put in a Teflon vessel and placed in an oven at 160

°C for 3 h to perform the hydrothermal process. In the hydrothermal process, the mixed urea-Gly gradually leavened to send out OH⁻, and the produced OH⁻ was connected with the metal ions to form precipitates. Then, the residual solution (containing urea and Gly) and precipitate were directly transferred to a porcelain crucible to continue a combustion reaction in a furnace at 500 °C. In the combustion process, the urea-Gly acts as fuel to ignite the reactant. After the combustion reaction was completed, the resulting precursor powders appeared to be pale-yellow foam with swelling. Finally, the precursor powders were grounded with an agate mortar, and moved to a corundum crucible to heat-treatment at different temperatures (900–1200 °C) for 3 h.

2.2 Characterization

The X-ray powder diffraction (XRD) patterns of the samples were obtained using an X-ray diffractometer (BrukerD8Advance, Germany) with CuK α ($\lambda= 1.5406 \text{ \AA}$) radiation at 40 kV and 40 mA over a 2θ scan range of 15–65°. The morphology, particle size, energy dispersive X-ray spectroscopy (EDS) and the mapping elements of the powders were studied using a field emission scanning electron microscope (SEM, S-4800 Hitachi, Japan). The photoluminescence excitation and emission spectra were measured using a spectrofluorometer (F-4600 Hitachi, Japan) equipped with a Xe lamp as the excitation source, and both the excitation and emission slits were 2.5 nm. The fluorescent decay curves and lifetimes were recorded using a spectrofluorometer (FS5-TCSPC Edinburgh, the United Kingdom). All the measurements were carried out at room temperature.

3. Results and discussion

3.1 The structural and morphological characterization

To investigate the composition and the effects of urea-Gly content as well as the post-sintering temperature on the crystallization of the powders, the XRD patterns of some samples were carried out and given in Figs. 1 and 2. Fig. 1 shows the XRD patterns of the phosphor samples assisted with different molar ratios of urea to Gly (5 : 1~5) heat-treated at the same temperature (1000 °C) for 3 h. In Fig. 1, the diffraction peaks at 16.8°, 29.1°, 29.8°, 30.2°, 42.1° and 53.1° correspond to the (110), (220), (130), (111), (221) and (151) planes of Sr₂CeO₄, respectively, which are in agreement with the JCPDS 50-0115 and indicate the formation of Sr₂CeO₄ after heat-treatment at 1000 °C no matter what molar ratio of urea to Gly is used. However, the intensities of diffraction peaks closely depend on the molar ratio of urea to Gly. Without the addition of Gly, the diffraction peaks are all very

weak, which implies the sample is not well-crystallized. After the addition of Gly, the peak intensities get obviously stronger as the molar ratio of urea to Gly reaches 5:2. Further increase the molar ratio of urea to Gly to 5:5 still remains good crystallization. This phenomenon convinces us that the Gly plays a crucial role in improving the crystallization of the samples. Additionally, one weak peak around 20.7° is observed in Fig. 1, which should originate from SrCeO_3 [18]. In other words, a small quantity of SrCeO_3 is simultaneously formed during the preparation of Sr_2CeO_4 . It can be found that the impurity peak intensity from SrCeO_3 is somewhat increased with the increase of molar ratio of urea to Gly from 5:2 to 5:5, but the peak intensity corresponding to (110) of Sr_2CeO_4 is oppositely decreased. As a result, the optimal content of urea to Gly for preparing pure Sr_2CeO_4 should be 5:2.

Fig. 2 shows the XRD patterns of the precursor powders and the samples prepared by heat-treatment from 900–1200 °C (the molar ratio of urea to Gly keeps the same as 5:2). For the precursor powders, the Sr_2CeO_4 is not formed and most of the XRD peaks correspond to $\text{Sr}(\text{NO}_3)_2$, SrCO_3 , and CeO_2 (labeled with #, o and Δ in Fig. 2, respectively). After heat-treatment with 900 °C, the Sr_2CeO_4 composition can be achieved. However, quite a few diffraction peaks belonging to SrCO_3 and CeO_2 still exist in the samples, which confirms that 900 °C as heat-treatment temperature is not suitable to obtain pure Sr_2CeO_4 . As the heat-treatment temperature is increased to 1000 °C, the peaks ascribed to SrCO_3 and CeO_2 are almost vanished, and the pure Sr_2CeO_4 should be achieved. Further increase the sintering temperature to 1100–1200 °C, the diffraction peak intensities are also increased, implying that the host crystallization can be well-improved by adjusting the post-sintering temperatures.

In order to further explore the composition and elemental distribution of the products, the EDS and elemental mappings for the sample prepared with urea-Gly (the molar ratio of urea: Gly = 5:2) assisted hydrothermal combustion reaction and subsequent heat-treatment at 1100 °C are measured and shown in Fig. 3. The result reveals the existence of Sr, Ce, and O elements, and no other elements are observed in the spectra (Fig. 3a). Additionally, the product shows a homogenous distribution of the elements (Sr, Ce and O for Fig. 3b-d, respectively), manifesting that the pure Sr_2CeO_4 sample can be achieved.

The morphology and size of the Sr_2CeO_4 samples prepared at different conditions were analyzed with SEM and displayed in Fig. 4. Without the addition of Gly in the synthesis process of

precursors (Fig. 4a), the samples after heat-treatment at 1000 °C are still poor-crystallized and the particles seem to be serious agglomeration with irregular distribution. Nevertheless, the particle crystallization and surface morphology are dramatically improved when the mixed urea and Gly are used in the hydrothermal combustion reaction. Fig. 4(b-d) gives the SEM images of samples after sintering with different temperatures (900–1100 °C) in which the molar ratio of urea to Gly is the same as 5:2. As the sintering temperature is 900 °C (Fig. 4b), most of the particles are crystallized with the particle size around 50~250 nm (not very homogenous). With the increase of heat-treatment temperature to 1000 °C (Fig. 4c), the samples exhibit well-crystallized spherical shape and the agglomeration phenomena are greatly decreased. Simultaneously, the particle looks uniform and the size is about 80~150 nm. Further increasing of the heat-treatment temperature to 1100 °C leads to much stronger crystallization and enlarged particle size (200~350 nm), as can be seen from Fig. 4d.

The above XRD and SEM results all confirm that Gly acts as an important role in the preparation process of Sr₂CeO₄ samples. Without the addition of Gly, the XRD diffraction peak intensities are very weak (Fig. 1, urea:Gly = 5:0) and therefore results in poor crystallization (Fig. 4a). After certain amount of Gly is introduced into the hydrothermal combustion reactions, the XRD diffraction peak intensities (such as Fig. 1, urea:Gly = 5:2) are greatly enhanced and the strong crystallization is formed (Fig. 4c and d). This means that Gly is not only a leavening agent and fuel but also an effective surfactant to control the crystal growth and particle distribution. On the other hand, the post-sintering temperature is also an important factor to influence the host composition, crystal growth as well as the surface shape. At relative low heat-treatment temperature (900 °C), there still exists quite a few SrCO₃ and CeO₂ impurities. By increasing the sintering temperature to 1000–1100 °C, the relative pure Sr₂CeO₄ can be achieved and display well-crystallized spherical shape.

In general, the spherical morphology, small degree of agglomeration and uniform particle size play the crucial roles for the phosphor powders in practical applications [19]. Therefore, it is necessary to investigate in detail on the luminescence properties of the well-distributed uniform spherical Sr₂CeO₄ powders.

3.2 The photoluminescence properties

The photoluminescence properties of the Sr_2CeO_4 powders prepared with different molar ratio of urea to Gly (the sintering temperature is $1000\text{ }^\circ\text{C}$) were measured and given in Fig. 5 and Fig. 6, respectively. The excitation spectra (Fig. 5) mainly consist of a broadband with peak at 277 nm , corresponding to the charge transfer transition from oxygen (O) to Ce^{4+} [20]. The emission spectra (Fig. 6) excited with 277 nm also present a broadband with maximum at 468 nm , which is ascribed to the transition from ligand-to-metal Ce^{4+} charge transfer state to the ground state and almost the same as those reported by a few groups [7,9,10]. Therefore, the Sr_2CeO_4 powders prepared by hydrothermal combustion reaction can generate the characteristic blue-light emission under the excitation with UV light. However, the emission peak is quite different from that Danielson's result (485 nm) [5]. The reason for the large peak shift should be due to the difference of the preparation methods and particle sizes [7,21]. On the other hand, the luminescence intensity is closely related to the molar ratio of urea to Gly, as can be seen from Figs. 5 and 6. When the molar ratio of urea to Gly varies from 5:0 to 5:2, the blue-light emission intensity also gradually increases. After further increase the content of Gly, the emission intensity of the Sr_2CeO_4 sample decreases inversely. The reason for this is that Gly not only acts as fuel but also as surfactant in the reaction. As surfactant, the appropriate Gly can serve as capping agent to improve the crystallization, particles distribution and morphology. However, the introduction of excessive Gly will form micelles and lead to serious particle aggregations with dense pores after combustion process [22]. The facts support the conclusion that the amount of Gly is an important factor in enhancing the luminescence intensity and the optimal molar ratio of urea to Gly is 5:2, which is quite consistent with the above XRD and SEM analysis. In other words, the optimal molar ratio of urea to Gly can not only lead to strong crystallization and regular particle distribution, but also improve the luminescence efficiencies.

Since the post-sintering temperature to the precursor of the samples evidently influenced the crystal structure and morphology (Fig.2 and Fig. 4), the photoluminescence properties of Sr_2CeO_4 after heat-treatment at different temperatures were further investigated, and the emission spectra (the molar ratio of urea to Gly is 5:2) are shown in Fig. 7. Under the excitation with UV light, the samples all exhibit characteristic blue-light emission at 468 nm , and the luminescence intensity is obviously enhanced with the increase of the sintering temperature from 900 to $1100\text{ }^\circ\text{C}$. At relative low heat-treatment temperature $900\text{ }^\circ\text{C}$, there exists some impurities including SrCO_3 and CeO_2 , and the particles are not well-crystallized. Therefore, the sample shows very weak emission

intensity. With the increase of sintering temperature to 1000–1100 °C, the impurities are obviously vanished and the particles display superior crystallization and uniform shape, which results in the dramatically enhanced luminescence. The relative emission intensity of the samples after sintering at 1100 °C is more than 2-fold as compared to that heat-treated at 900 °C. As the sintering temperature further increases to 1200 °C, the blue-light emission intensity decreases due to the formation of harder particles and coarser surface [23]. In consequence, the optimal sintering temperature to achieve strong blue-light emission should be 1100 °C. The diagram of CIE chromaticity coordinates (achieved from the strongest emission line of Fig. 7) as well as the luminescence photograph (irradiated with a 254 nm UV lamp) of the optimized Sr₂CeO₄ sample is given in Fig. 8. The CIE chromaticity coordinates of the optimized sample are $x = 0.17$ and $y = 0.23$, which shows blue-white emission and is better than in reference 4.

Fig. 9 gives the excitation spectra of the sample after heat-treatment at 1100 °C. In Fig. 9, there is a wideband from 200 to 400 nm (red line) and the strong peak locates at 277 nm, which is almost the same as previously described in Fig. 5. Moreover, a shoulder peak at about 350 nm can also be easily noticed. To clearly elucidate the excitation spectra, the original broadband is separated into two peaks by deconvolution means. One is the main peak at 277 nm (green line), and the other is at 350 nm (black line). It is known that in orthorhombic Sr₂CeO₄, each Ce atom is coordinated with six O atoms. The octahedron shows two trans-terminal Ce-O1 perpendicular to the plane defined by four equatorial O2 atoms. Therefore, the two excitation peaks should be attributed to the different charge transfer transitions from O to Ce⁴⁺. Actually, a tiny shoulder peak at 350 nm also exists in Fig. 5, but it is so weak as compared to the main peak at 277 nm. The results indicate that the Sr₂CeO₄ sample after sintering at 1100 °C can both be effectively excited with medium and near ultraviolet light. This may be a good hint for its practical uses in optoelectronic industry.

The nature of the luminescent decay kinetics of orthorhombic Sr₂CeO₄ has ever been studied by Van Pieterse group [20]. To further investigate the luminescence behavior and achieve the decay lifetimes of Sr₂CeO₄ fine phosphor powders prepared by hydrothermal combustion, the luminescent decay curves of the optimized sample were measured and shown in Fig. 10. The decay curve for the fine powders is well fitted with a single-exponential function, implying that the Ce⁴⁺ ion in the lattice should locate only one type of site. The decay lifetime τ is about 35.8 μ s, which is almost the same as Van Pieterse reported (35 μ s) and shorter than Danielson's result (50 μ s). In Sr₂CeO₄

crystal, the Ce^{4+} ion has empty 4f shell. One electron from oxygen ligand can be transferred to the 4f shell of Ce^{4+} and result in the ligand–metal charge transfer transition. Due to a relatively long decay lifetime ($\sim\mu\text{s}$), the charge transfer is not possible to be a spin-allowed transition. Therefore, it should be a spin-forbidden transition and produce a high spin triplet excited state.

4. Conclusion

The Sr_2CeO_4 phosphor powders with orthorhombic system have been successfully prepared through hydrothermal combustion reaction and a heat-treatment process. In the reaction process, the urea and Gly components are both mixed into the raw materials as leavening agent and fuel. It has been found that the molar ratio of urea to Gly and the post-sintering temperature are very important factors to adjust and improve the particle crystallization, surface morphology and luminescence intensities of the Sr_2CeO_4 phosphor powders. The optimized molar ratio of urea to Gly as well as the sintering temperature is confirmed to be 5:2 and 1100 °C, respectively. In the post-sintering process, the reduction atmosphere is not necessary, and the optimized sintering temperature to achieve the fine Sr_2CeO_4 powder is much lower than 1400–1600 °C. After optimization, the samples display not only strong crystallization and well-distributed spherical particle, but also intense blue-light emission as excited with medium (277 nm) and near ultraviolet light (350 nm). The luminescence decay time is about 35.8 μs , and the CIE chromaticity coordinates are $x = 0.17$ and $y = 0.23$. The hydrothermal combustion synthesis is an effective approach to achieve fine Sr_2CeO_4 phosphor powders (200~350 nm), which may be beneficial to the practical applications in the optoelectronic fields.

Acknowledgments

This work was financially supported by Natural Science Foundation of Hebei Province (Grant No. E2015205159), China, Science Foundation of Hebei Education Department (Grant No. ZD2014045), China, High Level Talents Foundation in Hebei Province (Grant No. C201400327), China, and the Science Foundation of Hebei Normal University (Grant No. L2013K02), China. This work was also developed within the scope of the project CICECO-Aveiro Institute of Materials,

POCI-01-0145-FEDER-007679 (FCT Ref. UID/CTM/50011/2013), financed by national funds through the FCT/MEC and when appropriate co-financed by FEDER under the PT2020 Partnership Agreement.

References

- [1] H. A. Höpfe, Recent developments in the field of inorganic phosphors, *Angew. Chem. Int. Ed.* 48 (2009) 3572–3582.
- [2] Z.G. Xia, C.G. Ma, M.S. Molokeev, Q.L. Liu, K. Rickert, K.R. Poeppelmeier, Chemical unit cosubstitution and tuning of photoluminescence in the $\text{Ca}_2(\text{Al}_{1-x}\text{Mg}_x)(\text{Al}_{1-x}\text{Si}_{1+x})\text{O}_7:\text{Eu}^{2+}$ Phosphor, *J. Am. Chem. Soc.* 137 (2015) 12494–12497.
- [3] A. Lacanilao, G. Wallez, L. Mazerolles, V. Buissette, T.L. Mercier, F. Aurissergues, Marie-F. Trichet, N. Dupre, B. Pavageau, L. Servant, B. Viana, A structural approach of the flux effect on blue phosphor BAM: Eu ($\text{BaMgAl}_{10}\text{O}_{17}:\text{Eu}^{2+}$), *Mater. Res. Bull.* 48 (2013) 2960–2968.
- [4] E. Danielson, M. Devenney, D.M. Giaquinta, J.H. Golden, R.C. Haushalter, E.W. McFarland, D.M. Poojary, C.M. Reaves, W. H. Weinberg, X.D. Wu, A rare-earth phosphor containing one-dimensional chains identified through combinatorial methods, *Science* 279 (1998) 837–839.
- [5] E. Danielson, M. Devenney, D.M. Giaquinta, J.H. Golden, R.C. Haushalter, E.W. McFarland, D.M. Poojary, C.M. Reaves, W. H. Weinberg, X.D. Wu, X-ray powder structure of Sr_2CeO_4 : a new luminescent material discovered by combinatorial chemistry, *J. Mol. Struct.* 470 (1998) 229–235.
- [6] Y. D. Jiang, F. Zhang, C.J. Summers, Z.L. Wang, Synthesis and properties of Sr_2CeO_4 blue emission powder phosphor for field emission displays, *Appl. Phys. Lett.* 74 (1999) 1677–1679.
- [7] L. Li, S.H. Zhou, S.Y. Zhang, Investigation on charge transfer bands of Ce^{4+} in Sr_2CeO_4 blue phosphor, *Chem. Phys. Lett.* 453 (2008) 283–289.
- [8] M. Stefanski, L. Marciniak, D. Hreniak, W. Strek, Size and temperature dependence of optical properties of $\text{Eu}^{3+}:\text{Sr}_2\text{CeO}_4$ nanocrystals for their application in luminescence thermometry, *Mater. Res. Bull.* 76 (2016) 133–139.

- [9] D.L. Monika, H. Nagabhushana, S.C. Sharma, B.M. Nagabhushana, R. Hari Krishna, Synthesis of multicolor emitting $\text{Sr}_{2-x}\text{Sm}_x\text{CeO}_4$ nanophosphor with compositionally tunable photo and thermoluminescence, *Chem. Engin. J.* 253 (2014) 155–164.
- [10] T. Grzyb, A. Szczeszak, J. Rozowska, J. Legendziewicz, S. Lis, Tunable luminescence of $\text{Sr}_2\text{CeO}_4:\text{M}^{2+}$ (M = Ca, Mg, Ba, Zn) and $\text{Sr}_2\text{CeO}_4:\text{Ln}^{3+}$ (Ln = Eu, Dy, Tm) nanophosphors, *J. Phys. Chem. C* 116 (2012) 3219–3226.
- [11] R. Ghildiyal, P. Page, K.V.R. Murthy, Synthesis and characterization of Sr_2CeO_4 phosphor: Positive features of sol–gel technique, *J. Lumin.* 124 (2007) 217–220.
- [12] D.L. Monika, H. Nagabhushana, B.M. Nagabhushana, S.C. Sharma, K.S. Anantharaju, B. Daruka Prasad, C. Shivakumara, One pot auto-ignition based synthesis of novel $\text{Sr}_2\text{CeO}_4:\text{Ho}^{3+}$ nanophosphor for photoluminescent applications, *J. Alloys. Compd.* 648 (2015) 1051–1059.
- [13] X.M. Liu, Y. L. J. Lin, Synthesis and characterization of spherical Sr_2CeO_4 phosphors by spray pyrolysis for field emission displays, *J. Cryst. Growth* 290 (2006) 266–271.
- [14] C.H. Lu, T.Y. Wu, C.H. Hsu, Synthesis and photoluminescent characteristics of Sr_2CeO_4 phosphors prepared via a microwave-assisted solvothermal process, *J. Lumin.* 130 (2010) 737–742.
- [15] J.L. Ferrari, A.M. Pires, O.A. Serra, M.R. Davolos, Luminescent and morphological study of Sr_2CeO_4 blue phosphor prepared from oxalate precursors, *J. Lumin.* 131 (2011) 25–29.
- [16] X. Yang, Z.B. Shao, H.Q. Ru. Preparation and characterisation of $\text{Sr}_2\text{CeO}_4:\text{Eu}^{3+}$ rare earth luminescent material by high temperature mechano-chemical method, *J. Mater. Sci. Technol.* 32 (2016) 1066–1070.
- [17] T. Hirai, Y. Kawamura, Preparation of Sr_2CeO_4 blue phosphor particles and rare earth (Eu, Ho, Tm, or Er)-doped Sr_2CeO_4 phosphor particles, using an emulsion Liquid Membrane System, *J. Phys. Chem. B* 108 (2004) 12763–12769.
- [18] S.K. Gupta, M. Sahu, K. Krishnan, M. K. Saxena, V. Natarajana, S. V. Godbole, Bluish white emitting Sr_2CeO_4 and red emitting $\text{Sr}_2\text{CeO}_4:\text{Eu}^{3+}$ nanoparticles: optimization of synthesis parameters, characterization, energy transfer and photoluminescence, *J. Mater. Chem. C* 1 (2013) 7054–7063.
- [19] N.O. Nuñez, S.R. Liviano, M. Ocaña, Citrate mediated synthesis of uniform monazite LnPO_4 (Ln = La, Ce) and $\text{Ln}:\text{LaPO}_4$ (Ln = Eu, Ce, Ce + Tb) spheres and their photoluminescence, *J.*

Colloid Interf. Sci. 349 (2010) 484–491.

- [20] L. van Pieterse, S. Sovarna, A. Meijerink, On the nature of the luminescence of Sr₂CeO₄, J. Electrochem. Soc. 147 (2000) 4688–4691.
- [21] M. Stefanski, L. Marciniak, D. Hreniak, W. Streck, Influence of grain size on optical properties of Sr₂CeO₄ nanocrystals, J. Chem. Phys. 142 (2015) 184701.
- [22] S.K. Shi, D. Wei, K.Y. Li, S.P. Wang, L.S. Fu, T. Yang, L.J. Meng, Combustion synthesis of Ce₂LuO_{5.5}:Eu phosphor nanopowders: structure, surface and luminescence investigations, Appl. Surf. Sci. <https://doi.org/10.1016/j.apsusc.2018.03.060>.
- [23] T. Li, C.F. Guo, Y.R. Wu, L. Li, J.H. Jeong, Green upconversion luminescence in Yb³⁺/Er³⁺ co-doped ALn(MoO₄)₂ (A= Li, Na, and K; Ln=La, Gd and Y), J. Alloys. Compd. 540 (2012) 107–112.

Figure captions

Fig. 1. The XRD patterns of the powders prepared with hydrothermal combustion reaction in different molar ratios of urea to Gly (the sintering temperature is 1000 °C).

Fig. 2. The XRD patterns of the precursor powders and samples after a sintering process at different temperatures (the molar ratio of urea to Gly is 5:2).

Fig. 3. The EDS spectra (a) and elemental mappings of Sr (b), Ce(c) and O(d) of Sr₂CeO₄ powders.

Fig. 4. The SEM images of Sr₂CeO₄ powders after sintering at (a) 1000 °C without Gly, (b) 900 °C, (c) 1000 °C, and (d) 1100 °C with Gly.

Fig. 5. The excitation spectra ($\lambda_{em}= 468$ nm) of Sr₂CeO₄ powders prepared with hydrothermal combustion reaction in different molar ratios of urea to Gly (sintering temperature is 1000 °C).

Fig. 6. The emission spectra ($\lambda_{ex}= 277$ nm) of Sr₂CeO₄ powders prepared with hydrothermal combustion reaction in different molar ratios of urea to Gly (sintering temperature is 1000 °C).

Fig. 7. The dependence of emission spectra ($\lambda_{ex}= 277$ nm) of Sr₂CeO₄ powders with the post-sintering temperature (the molar ratio of urea to Gly is 5:2).

Fig. 8. The diagram of CIE chromaticity coordinates (achieved from the strongest emission line of Fig. 7) and the luminescence photograph (irradiated with a 254 nm UV lamp) of the optimized Sr₂CeO₄ sample.

Fig. 9. The excitation spectra ($\lambda_{em}= 468$ nm) of Sr₂CeO₄ powders prepared with hydrothermal combustion reaction (the molar ratio of urea to Gly is 5:2) and heat-treatment at 1100 °C.

Fig. 10. The luminescence decay curve of the O–Ce charge transfer transition for Sr₂CeO₄ powders.

Fig 1

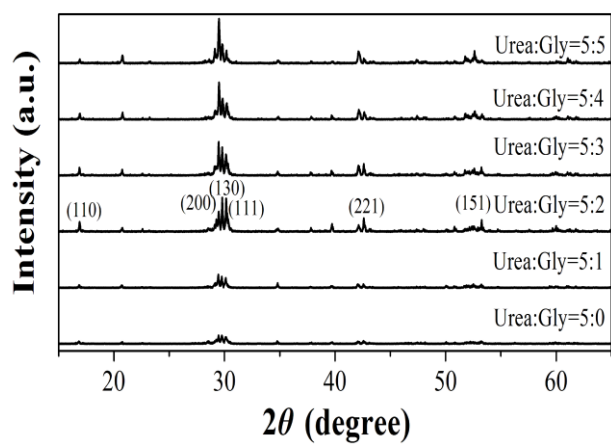


Fig 2

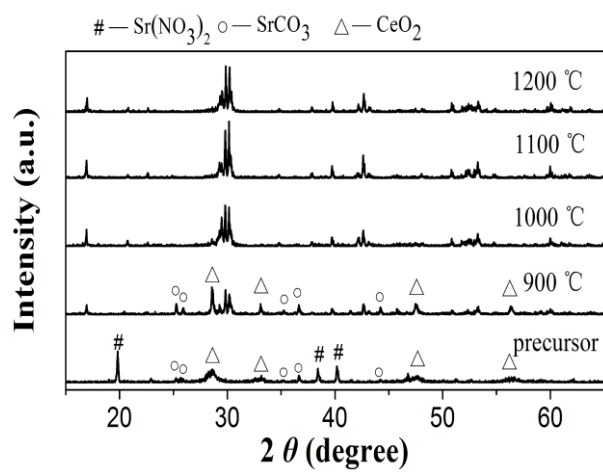


Fig 3

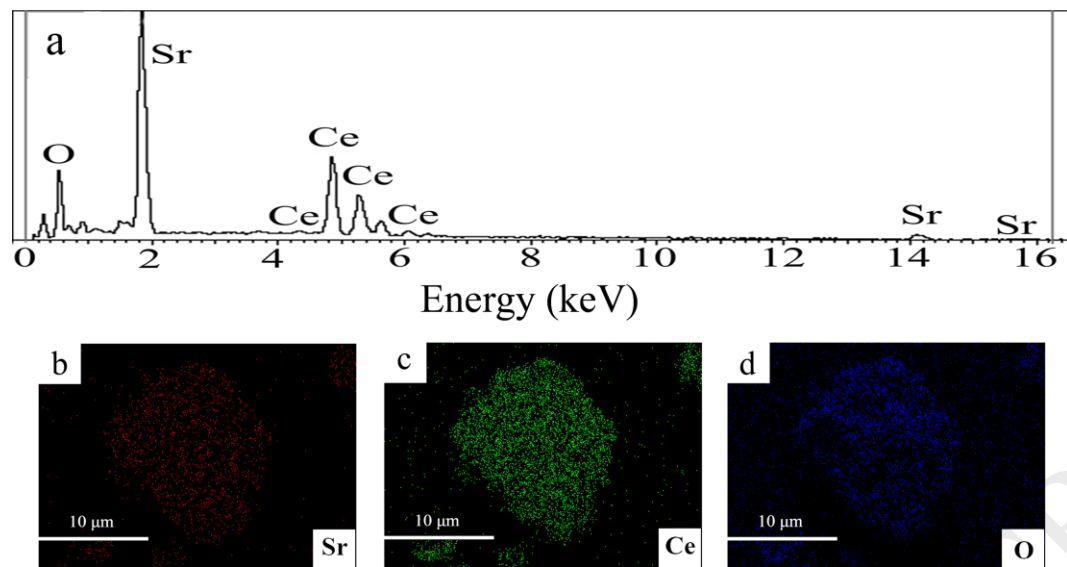


Fig 4

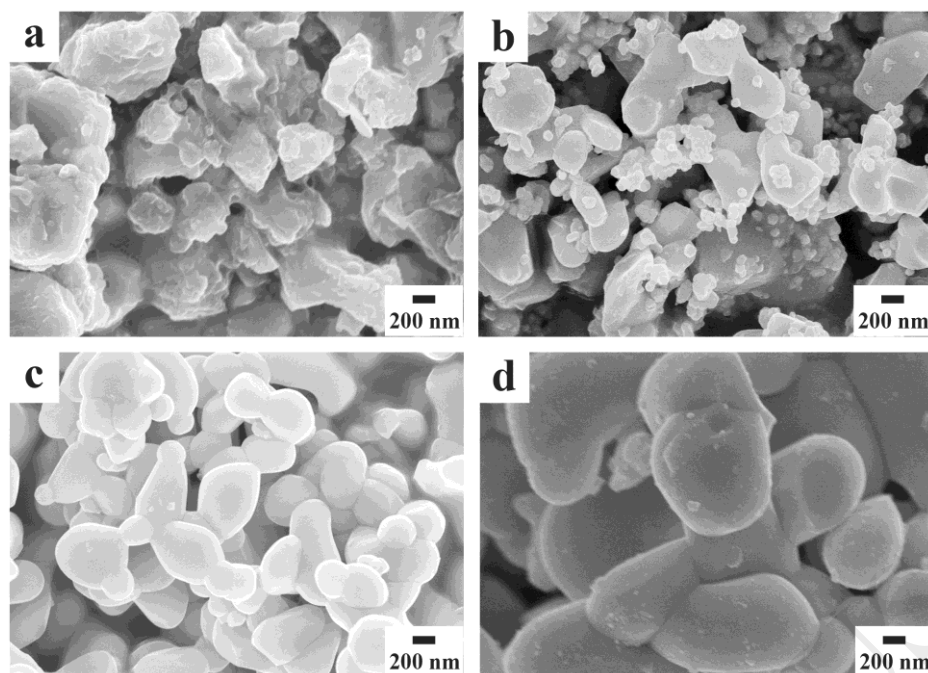


Fig 5

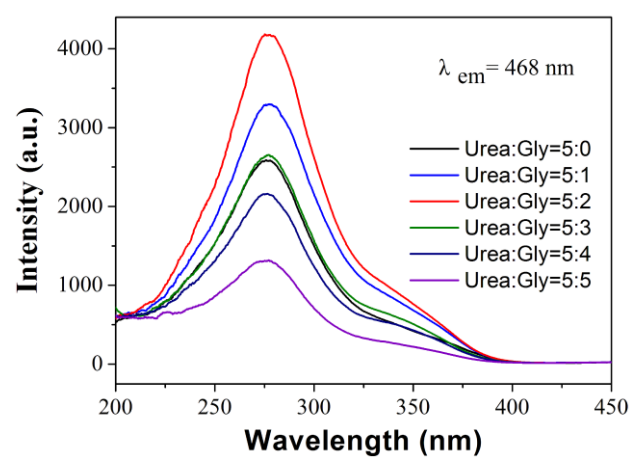


Fig 6

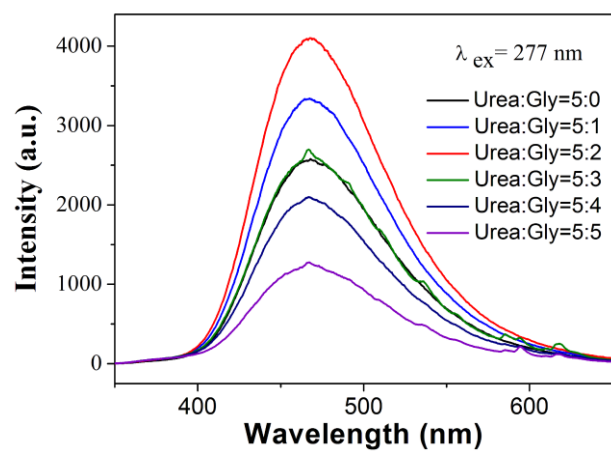


Fig 7

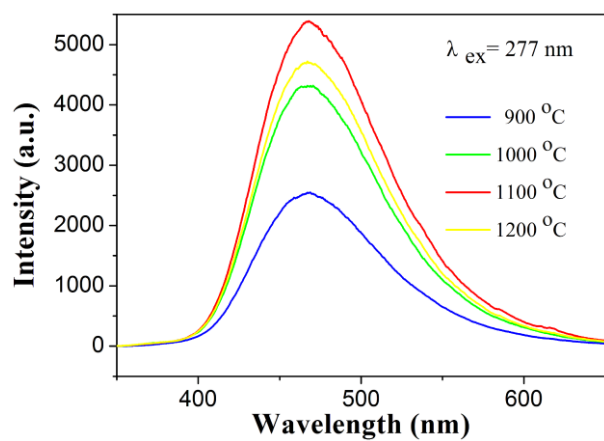


Fig 8

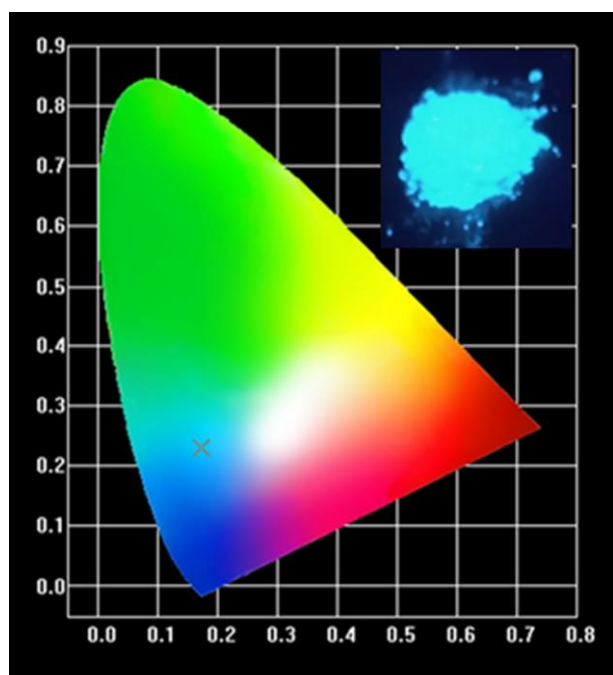


Fig 9

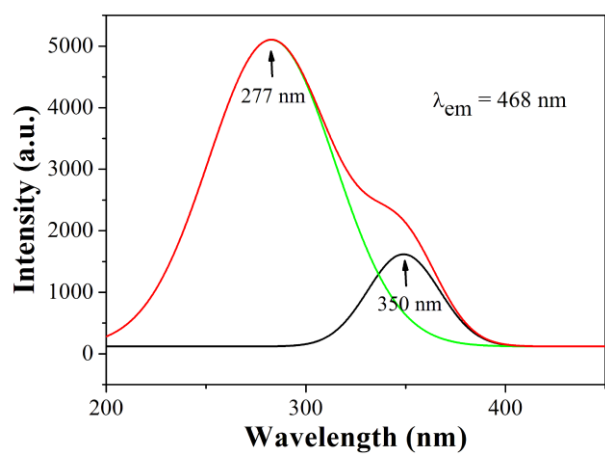


Fig 10

